Management Systems in Production Engineering

2026, Volume 34, Issue 1, pp. 120-126

Date of submission of the article to the Editor: 05/2025
Date of acceptance of the article by the Editor: 01/2026

DOI 10.2478/mspe-2026-0012

ADVANCED ELECTROCHEMICAL DISCHARGE MACHINING AND PROCESS OPTIMIZATION FOR HYBRID METAL MATRIX COMPOSITES

Safa M. Lafta, Abbas F. Ibrahim
University of Technology, Baghdad

Abstract:
Composite and non-conductive materials are machined using an advanced technology known as electrochemical discharge machining (ECDM). This paper investigates the machinability of an aluminum 6061 alloy reinforced with boron carbide (B4C) and silicon carbide (SiC) HMMCs. It investigates how voltage, electrolyte concentration, and pulse-on and pulse-off periods affect the Material Removal Rate (MRR). An ANOVA (analysis of variance) revealed that the most significant factor was voltage (F-value = 36.61, P-value = 0.004), followed by pulse-on time (Pon), with electrolyte concentration and pulse-off time (Poff) having little impact. Regression analysis (adjusted R^2 = 74.18%) demonstrated model dependability. Increasing the voltage and pulse-on time enhances MRR, machining efficiency, and stability. This paper presents a statistically proven optimization strategy for aerospace and automotive applications.

Key words: Electrochemical Discharge Machining (ECDM), Hybrid Metal Matrix Composite (HMMCs), Material Removal Rate (MRR), process optimization

INTRODUCTION

Combining electrochemical machining (ECM) and electrical discharge machining (EDM) [1] offers benefits such as reduced heat-affected zones (HAZ), lower skill requirements, and no external force for material removal. The downsides include electrode wear, overcutting, uncontrolled sparks, and harmful fume emissions [2, 3]. This study employs ECDM to evaluate the machinability of Al 6061-S_iC-B_4C composites, with the purpose of optimizing crucial factors, including pulse duration and voltage, and determining their effects on thermal impact, surface finish, and machining performance [4]. Composites made of aluminum have many useful properties, such as increased hardness, reduced thermal expansion coefficient, high strength, and excellent resistance to wear and tear. Metal matrix composites are challenging to machine using traditional machines due to their high hardness and reinforcement strength [5, 6]. The wear resistance, strength-to-weight ratio, and HMMCs standing for thermal stability of HMMCs, which are typically composed of Al 6061 reinforced with S_iC and B_4C, make them indispensable in many industrial, automotive, aerospace, and defense sectors [7, 8, 9]. Aluminum is reinforced with abrasive particles made of high-hardness silicon, boron carbide, or aluminum oxide. Sizes ranging from 10 µm to 100 µm are possible for the reinforcing material. Reinforcement impingement improves the base matrix's mechanical, tribological, and physical qualities [10, 11]. By increasing ECDM efficiency, the researchers seek to increase process control and product quality. Investigated the ECM of titanium alloy Ti-6Al-4V-ELI employing various electrolytes. The research evaluates the impact of electrolyte type on surface roughness (Ra), *MRR*, and machining accuracy. Key findings show that electrolyte composition significantly affects ECM performance, with sodium chloride (NaCl) and sodium nitrate ($NaNO_3$) mixtures providing optimal results with regard to better surface finish and higher MRR. The study highlights the potential of ECM as a non-traditional machining method for hard-to-machine biomedical alloys like Ti-6Al-4V-ELI [12]. The effectiveness of EDM on AA6061 HMMCs reinforced with S_iC and aluminum oxide (Al_2O_3) was investigated, and process parameters were examined for their effects on *MRR* and Ra using a Taguchi design and (ANOVA). The two most important variables were Pon and peak current. The study provides optimized EDM conditions for improved machinability of HMMCs [13]. Investigated voltage's effects, inter-electrode gap (IEG), and electrolyte concentration (NaCl) on the ROC, which is radial overcut and *MRR*, which is the material removal rate in Al-7.5% B_4C ECM. The outcomes indicated that increasing the voltage and electrolyte content improved both ROC and *MRR* [14]. Examined ECM factors such feed rate, voltage, and electrolyte content when milling Al5086/flyash/S_iC HMMCs and found that *MRR* rose with feed rate and voltage while electrolyte concentration had less of an effect [15]. Examined the impact of discharge current on *MRR*, which stands for *MRR*, and electrode wear rate (EWR), which stands for (EWR) in powder-mixed EDM and EDM for B_4C-reinforced Al2014 MMCs. Powder was employed to lower EWR, increase WRR, and improve machining stability [16]. Evaluated the Wire EDM (WEDM) of recycled Al alloy MMC with 5% alumina reinforcement, focusing on Pon, voltage, current, feed rate, and Poff. ANOVA and Criteria Importance Through Intercriteria (CRITIC) analysis uncovered that 30 V, 120 µs Pon, 7 mm/min feed rate, 30 A current, and 70µs Poff are optimal values for high *MRR* and low SR [17]. Examined the influences of pulse-on length, current, and electrode gap on *MRR*, Ra, which stands for Ra, and TWR, which stands for tool wear rate (TWR) in EDM machining of Al7075/B_4C. Ra and *MRR* increased in proportion to the current [18]. Examined the usage of electrolytes mixed with sodium hydroxide (NaOH) and Al_2O_3 for powder-mixed ECDM (PMECDM) and micro-ECDM (µ-ECDM) in the machining of maraging steel. PMECDM proved the benefits of adding (Al_2O_3) powder, increasing *MRR* by 34% and decreasing SR by 21% [19]. Investigated the EDM performance of AZ61/7.5% B_4C nanocomposites with nano-S_iC particles, using various dielectric fluids. Taguchi-based complex proportional assessment (COPRAS) was applied to optimize parameters. Results indicate that dielectric type and nano-S_iC addition significantly influence material removal rate, surface finish, and TWR. Optimal EDM conditions were identified, enhancing machining efficiency and surface quality [20]. Investigated usage of Friction Stir Processing (FSP) to reinforce Al6061-T6 with micro-sized S_iC particles. Microhardness improved by 59.45% and ultimate tensile strength (UTS) by 38.29% when S_iC volume increased [21]. Al-8% S_iC-4% B_4C has outstanding mechanical qualities, however, it is difficult to remove material efficiently and uniformly using traditional machining methods. This work uses a Taguchi L9 orthogonal array and ANOVA to explore the ECDM process for these HMMCs, examining the electrolyte concentration combined effects on *MRR*, which stands for *MRR*, Poff, voltage, and Pon. Despite previous research, which concentrated on individual parameters, this work presents a multi-variable optimization strategy, resulting in a statistically proven framework for improving machine performance. The findings help to improve process efficiency, machining control, and manufacturing HMMCs, especially in aerospace and automotive applications.

EXPERIMENTAL WORK

Workpiece

Although aluminum alloy Al6061 is a valuable material that is commonly employed in engineering applications, including construction and transportation where remarkable mechanical characteristics, including hardness and tensile strength, are required, it was chosen as the basic material [22]. The reinforcing particles included silicon carbide (S_iC) and boron carbide (B_4C). Making these composites has several advantages, including increased specific strength, thermal conductivity, and wear resistance, as well as a decreased coefficient of thermal expansion [23]. Table 1 shows the aluminum alloy's chemical composition was determined by the Ministry of Industry and Minerals/State Company for Inspection and Engineering Rehabilitation (SIER) in Baghdad, Iraq.

Table 1
The Al6061 alloy's chemical composition determined by optical emission spectroscopy (OES)

Element	Weight%	Element	Weight%
Mn%	0.0009	V%	0.0165
Cu%	< 0.300	Ti%	0.0106
Fe%	0.117	Zn%	0.0030
Mn%	0.0009	V%	0.0165

Optical emission spectroscopy (OES) was employed to collect data for the overall chemical analysis. The mechanical and physical parameters that were studied at the Materials Engineering Department of the University of Technology in Baghdad, Iraq are shown in Table 2.

Table 2
Mechanical and physical characteristics of Al6061 base material

Property	Values	Unit
Melting temperature	585-650	°C
Hardness	108	HV
Ultimate tensile strength	305	MPa
Elongation	11.8	%
Poisson's ratio	0.32	-
Modulus of elasticity	68.5	GPa
Shear strength	205	MPa
Shear modulus	25.8	GPa
Density	2.705	g/cm³

The reinforcement particles

In this work, B_4C, which stands for boron carbide, and S_iC, which stands for silicon carbide, microparticles were selected as reinforcement materials to improve the Aluminum 6061 (Al6061) matrix mechanical properties. These reinforcements were utilized to form a HMMCs with improved hardness, wear resistance, and strength. These powders were analyzed using energy dispersive spectroscopy (EDS) for S_iC and B_4C, as shown in Tables 3 and 4, respectively.

Table 3
Elemental composition of S_iC reinforcement particles analyzed via Energy Dispersive X-ray Spectroscopy (EDS)

Element	Atomic%	Atomic% Error	Weight%	Weight% Error
O	25.6	0.5	21.8	0.4
C	38.9	0.9	24.9	0.5
Si	35.5	0.1	53.2	0.2

The particle size of S_iC and B_4C reinforcements in the aluminum HMMCs were analyzed using Field Emission

Scanning Electron Microscope (FE-SEM). The measured sizes ranged from 22.39 nm to 66.99 nm.

Table 4
Elemental composition of B_4C reinforcement particles analyzed via (EDS)

Element	Atomic%	Atomic% Error	Weight%	Weight% Error
B	92.2	1.7	87.7	1.6
O	6.5	0.7	9.1	1.0
Si	1.3	0.1	3.2	0.2

The nano-scale distribution of these reinforcements contributes to enhanced mechanical properties and improved load transfer efficiency in the composite matrix as shown in Figures 1 and 2, respectively. The EDS and FE-SEM analyses were conducted at al-Khoura Company, Baghdad, Iraq.

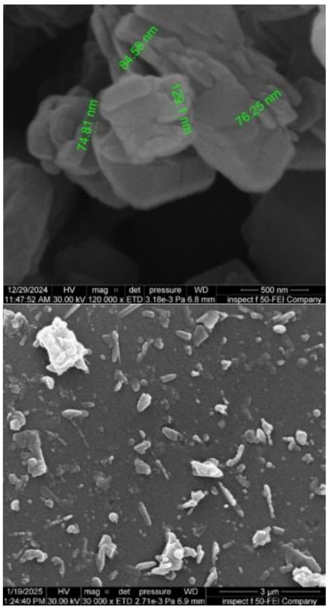

Fig. 1 Distribution and grain size of S_iC particles in Al6061 matrix as observed via FE-SEM

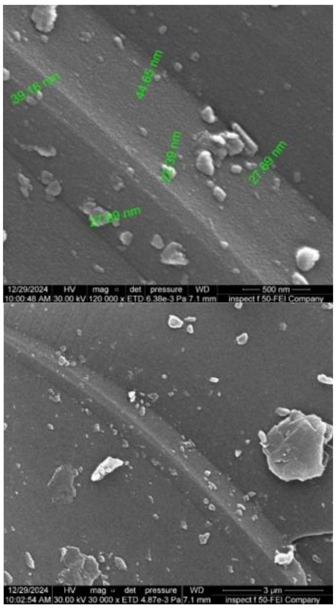

Fig. 2 Distribution and grain size of B_4C particles in Al6061 matrix as observed via FE-SEM

The stir-casting process

In present work, the basic matrix was Al6061 alloy, which was melted in a graphite crucible furnace at 750-800°C for 40-50 minutes to achieve total liquefaction. Aluminum Chloride Hexahydrate ($AlCl_3{\cdot}6H_2O$) was used as a degassing agent to eliminate trapped gasses and maintain homogeneous composition. To improve wettability and reduce porosity, reinforcement particles (S_iC and B_4C) were warmed in a muffle furnace at 600°C for an hour [24]. During stirring, a mechanical stirrer at 450 rpm created a vortex in the molten aluminum, ensuring uniform dispersion. The preheated particles were gradually introduced over 3-5 minutes, followed by an additional 10 minutes of continuous stirring for homogeneity. To further improve wettability, magnesium strips were added after slag removal, reducing surface tension and preventing blowhole formation [25]. To avoid thermal shock and manage cooling, the molten composite was immediately placed into a prepared graphite mold at 250°C. The solidification process lasted 40 minutes, reducing porosity and increasing structural integrity. To improve hardness and strength, the composite underwent quick water quenching followed by 6 hours of age at 180 degrees Celsius. The solidified workpiece was milled into specimens that measured 5 mm in thickness and 30 mm in diameter. This approach results in a well-dispersed reinforcement phase inside the aluminum matrix, which improves mechanical characteristics and structural endurance. Table 5 displays the chemical composition of Al-8% S_iC-4% B_4C that was examined at Al-Khoura company, Iraq / Baghdad, and Table 6 shows the mechanical properties of Al-8% S_iC-4 % B_4C that was examined in the Material Engineering Department at the University of Technology, Baghdad, Iraq.

Table 5
The chemical composition of Al-8% S_iC-4% B_4C hybrid composite material

Element	Atomic%	Atomic% Error	Weight%	Weight% Error
B	10.3	0.6	5.1	0.3
C	21.7	0.4	11.8	0.2
O	1.7	0.1	1.2	0.1
Si	0.6	0.0	0.8	0.0
Al	65.2	0.2	80.0	0.3
Mg	0.2	0.0	0.3	0.0
Fe	0.2	0.0	0.4	0.0
Zn	0.1	0.0	0.4	0.1

Table 6
The mechanical properties of Al-8% S_iC-4% B_4C composite material

Property	Values	Unit
Density	2.75	g/cm³
Elongation	10	%
Yield strength	110	MPa
Ultimate tensile strength	160	MPa
Modulus of elasticity	75	GPa
Hardness	160	HV

The additive S_iC and B_4C reinforcements substantially enhanced the hardness of Al-8%S_iC-4% B_4C from 108 HV (unreinforced Al6061) to 160 HV, enhancing mechanical strength through uniform ceramic particle distribution. This improvement, similar to findings by [21], benefits applications requiring high wear resistance and durability, such as aerospace and automotive components [21].

The electrode

The cylindrical copper electrode (10 mm diameter, 50 cm length) was employed in the machining process due to its high thermal conductivity, electrical conductivity, and simplicity of machining, as well as its availability, making it a practical choice in many industrial applications [26]. After each operation, the electrode was cleansed with water and dried to remove any stuck debris. After each process, the electrode was cleaned by washing it with water and drying it to remove any sludge adhered to its surface. Electrode copper was analyzed at the Ministry of Industry and Minerals/the State Corporation for Inspection and Engineering Rehabilitation (SIER) in Baghdad, Iraq, to identify its chemical composition, as stated in Table 7.

Table 7
Chemical composition of copper electrode used in ECDM

Element	Weight%
Zn%	0.0038
S%	0.0013
Al%	0.0152
As%	0.0007
Sb%	0.0121
Cr%	0.0008
Pb%	0.0011
Fe%	0.0482
P%	0.0007
Sn%	0.0025
Cu%	Bal.

Design and arrangement of the ECDM system

The ECDM was utilized to machine the HMMCs Al6061 reinforced with 8% wt. S_iC and 4% wt. B_4C, which was chosen for its ability to handle complex materials [27, 28, 29]. The ECDM setup includes an acrylic tank, a water pump, a copper electrode, a stainless-steel auxiliary electrode, a power source, and a computer. Furthermore, (NaCl) served as the electrolyte in this process. The tool represents the cathode during operation, while the workpiece represents the anode. The components of the ECDM system are illustrated in Figure 3 [2].

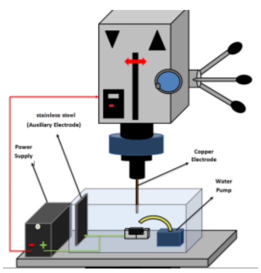

Fig. 3 The Schematic diagram of the ECDM setup, showing configuration including electrodes, electrolyte bath, and power supply
Source: [2].

Prior to each experiment, the electrode and workpiece were properly cleaned to remove any impurities. The workpiece was then securely placed in a stainless-steel holder. In addition, a 0.2 mm space was maintained between the workpiece and the tool.

Tests and inspections

The microstructure of the prepared cast specimens of the composites, which were Al 6061 with 8% SiC and 4% B_4C, was evaluated utilizing Scanning Electron Microscopy (SEM). Wet grinding was done using water and S_iC emery paper in grits of 320, 500, 600, 800, 1000, and 1200. The samples had been polished with a lubrication cloth and 0.5 µm diamond paste. The samples were then etched using Keller's reagent, which contained 1.5 mL of HCL, 2.5 mL of HNO3, 95 mL of H_2O, and 1.0 mL of HF. Figure 4 illustrates the SEM analysis, which highlights the key microstructural defects that affect mechanical properties, including crack propagation, porosity clustering, and reinforcement distribution.

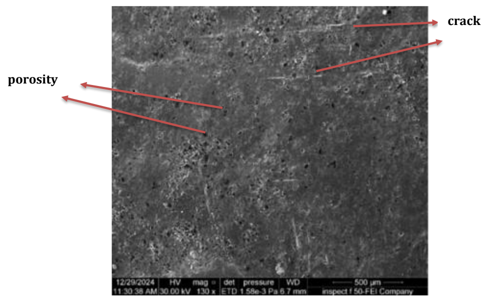

Fig. 4 SEM microstructure of Al-8% S_iC-4% B_4C composite showing defects like porosity and cracks

Optimization of processing parameters is essential to mitigate these defects. Figure 5 shows the base alloy aluminum 6061 with the distribution of particles (S_iC and B_4C). In this regard, the inspection was conducted at Al-Khoura Company in Baghdad, Iraq.

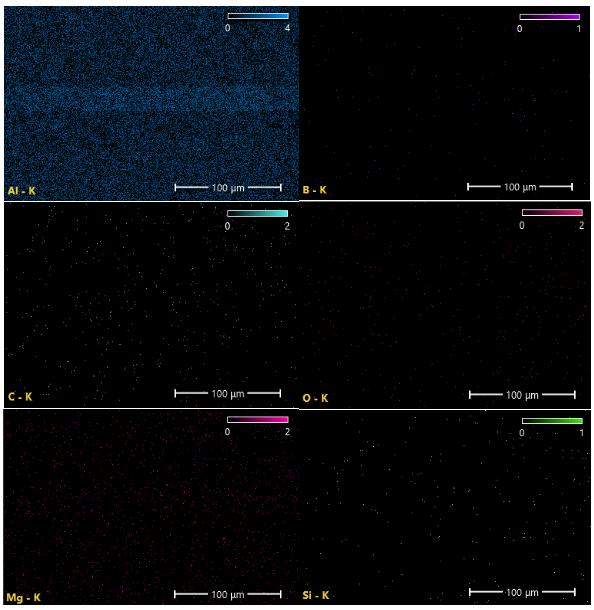

Fig. 5 Microstructure of base Al6061 showing reinforcement distribution of S_iC and B_4C particles

RESULTS OF RESEARCH

Following machining, the *MRR* can be computed by dividing the change in the workpiece's weight previous to and following machining by the time of machining, as presented in Eq. (1) [30]:

$$MRR = \frac{Wpb - Wpa}{MT}, \tag{1}$$

where:
Wpa refers to the workpiece's weight after machining (g),
MRR stands for the removal rate of material (g/min),
Wpb refers to the workpiece's weight prior to machining (g),
MT refers to the duration of machining (min), which was the same in all trials (3 minutes). Table 8 shows the experimental input parameters and levels used in Taguchi L9 design for ECDM of Al-8%S_iC-4%B_4C.

Table 8
The experimental input parameters and levels used in Taguchi L9 design for ECDM of Al-8%S_iC-4%B_4C

Parameters	Symbols	Levels		
		1	2	3
Concentrations % (Con.%)	X1	10%	20%	30%
Voltages (V)	X2	30	40	50
Poff (µsec)	X4	25	50	75
Pon (µsec)	X3	50	100	150

MINITAB 17 software was utilized to perform the nine tests that make up the design of experiments (DOE) for this study, which uses three stages based on the Taguchi orthogonal array design L9. This method was employed to assess the derived models' significance. More precisely, as shown in Table 9, each test comprised nine workpiece passes.

Table 9
Taguchi L9 experimental design matrix and measured MRR values for Al-8%S_iC-4%B_4C composite

No.	Con. %	V	Pon	Poff	MRR g/min
1	10	30	50	25	0.054
2	10	40	100	50	0.062
3	10	50	150	75	0.084
4	20	30	100	75	0.056
5	20	40	150	25	0.057
6	20	50	50	50	0.049
7	30	30	150	50	0.040
8	30	40	50	75	0.047
9	30	50	100	25	0.074

To ensure that no dirt, debris, or dielectric material remained after each operation of machining, thoroughly drying and cleaning the workpiece and electrode was performed. The Denver four-digit precision electronic balance, which measures from 0.0001-210 gm with an accuracy of 0.0001 gm, was used for the weighing. *MRR* was determined by weighing the workpiece previous to and following the machining process and factoring in the predicted time of machining.

DISCUSSIONS

The effect of *MRR*

MRR is a crucial element of ECDM and directly affects machining efficiency and productivity. In this study, through dividing the weight of workpiece difference before and after cutting by the amount of time spent machining, the *MRR* is calculated. Tables 10 and 11 contain the data applied to examine the various process factors' effect on *MRR*.

Table 10
ANOVA table showing the significance of input parameters on MRR during ECDM

Source	DF	Adj ss	Adj ms	F-Value	P-Value
Model	1	0.004839	0.004839	23.98	0.002
Linear	1	0.004839	0.004839	23.98	0.002
Voltage	1	0.004839	0.004839	23.98	0.0.002
Error	7	0.001413	0.000202		
Total	8	0.006252			

Table 11
Statistical model summary of regression fit for MRR prediction in ECDM process

S	R-sq	R-sq (adj)	R-sq (pred)
0.0142052	77.41%	74.18%	61.75%

Effect of voltage

The ANOVA, standing for Analysis of Variance, calculations in Table 10, showing that voltage (X2) is the most important factor impacting *MRR*. The F-value of 36.61 indicates statistical significance, as does the P-value of 0.004. *MRR* increases considerably when the voltage rises from 30V to 50V. This could be because each pulse removes more material due to the increased energy discharge. This finding is further confirmed by the regression equation in Table 11, which demonstrates a direct association between the voltage coefficient (0.001633) and *MRR*.

Effect of Pon

When determining *MRR*, Pon (X3) is essential. Table 9 illustrates that raising Pon from 50 µs to 150 µs yields a greater *MRR*. The regression analysis yielded a positive coefficient of 0.001092, indicating that longer energy application improves material removal.

Effect of electrolyte concentration

Electrolyte concentration (X1) has a beneficial, but less noticeable, effect on *MRR*. The regression coefficient (0.002540) implies a proportionate relationship, indicating that raising the concentration from 10% to 30% improves the electrolyte's conductivity, allowing for improved ion exchange and material removal.

Effect of Poff

Poff (X4) shows a relatively lower impact on *MRR*. The regression equation presents a small coefficient (0.001053), implying that while higher Poff allow better cooling and debris removal, their contribution to *MRR* remains minimal in comparison to voltage and Pon.

STATISTICAL ANALYSIS AND MODEL VALIDATION

The outcomes of ANOVA in Table 10 reveal that voltage is the most vital component, and after that comes Pon. The model summary in Table 5 uncovers an adjusted R-squared value of 74.18%, demonstrating a good connection between the experimental and regression data. The derived equation (Eq. 2) accurately predicts *MRR* based on input parameters, indicating its usefulness in optimizing ECDM processes. Eq. 2 represents the regression equation:

$$MRR = 0.0917 + 0.002540\,X1 - 0.002060\,X2 - 0.000971\,X3 + 0.001053\,X4 - 0.000052\,X1X4 + 0.000024\,X2X3 \quad (2)$$

Graphical representation of *MRR* trends

An assessment of the impacts of voltage and electrolyte concentration on pulse-on time, *MRR*, and Poff is presented in Figure 6. The graph confirms a strong linear increase in *MRR* with voltage, whereas the impacts of other parameters are relatively subdued. These findings suggest that optimizing voltage and Pon is essential for achieving greater *MRR* in ECDM of Al-8%S_iC-4%B_4C composites.

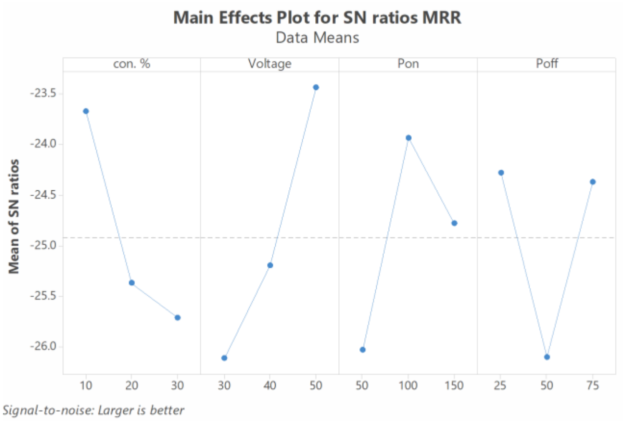

Fig. 6 Main effect plot illustrating the influence of process parameters on MRR in ECDM, including voltage, Pon, Poff, and electrolyte concentration

The study confirmed voltage as the most significant parameter influencing *MRR*, standing for Material Removal Rate in ECDM of Al-8%S_iC-4%B_4C, with ANOVA results (F-value = 36.61, P-value = 0.004) supporting its impact. This aligns with Gugulothu et al. (2022), who found voltage contributes 74% to machining efficiency [15]. Pon also increased *MRR* (50 to 150 µs), consistent with [18]. Electrolyte concentration had a smaller effect, corroborating [14], and Poff showed no effect, agreeing with [17]. Statistical validation guarantees dependable process optimization for aerospace and automotive applications.

CONCLUSION

This work demonstrated the effectiveness of ECDM for cutting Al-8%S_iC-4%B_4C HMMCs. Voltage was shown to be the most important parameter impacting *MRR*, with an F-value of 36.61 and a P-value of 0.004, followed by Pon. The modified parameters led to an improvement in hardness from 108 HV (base alloy) to 160 HV (reinforced composite), as well as a predictive regression model with an adjusted R^2 of 74.18%. Compared to prior studies, this work used a multi-variable optimization strategy based on Taguchi design and ANOVA to achieve higher machining efficiency and MRR while minimizing surface defects. The findings support the use of ECDM in high-performance applications such as aerospace and automotive manufacturing, where precision and material integrity are crucial. Comprehensive material characterization using (SEM) and (EDS) confirmed uniform reinforcement dispersion, reduced porosity, and minimal structural defects, supporting improved mechanical performance.

Future research is recommended to investigate nano-reinforcements, alternate electrolytes, or new machining control in HMMCs. Tool designs to improve *MRR*, surface quality, and machining control in HMMCs.

REFERENCES

[1] Özmen, U. & Asiltürk, İ. (2016). Electrochemical discharge machining: A review. *International Journal of Science and Engineering Applications 5*, pp. 495-499.

[2] Najm, V.N. (2024). *Investigation of surface integrity in electrochemical discharge machining (ECDM).* PhD Thesis, University of Technology, Baghdad, Iraq.

[3] Rajput, V., Goud, M. & Suri, N.M. (2021). Machinability study of spark assisted chemical engraving (SACE): A state of art. *Industrial Engineering Journal, 168*, pp. 2493-2513.

[4] Pundir, S.S., Goud, M. & Rajput, V. (2019). Micro-machining with ECDM: A state of art approach. *International Journal of Technical Innovation in Modern Engineering & Science, 5*, pp. 86-92.

[5] Ding, X., Liew, W. & Liu, X. (2005). Evaluation of machining performance of MMC with PCBN and PCD tools. *Wear, 259*, pp. 1225-1234. DOI: 10.1016/j.wear.2005.02.094

[6] Xavior, M.A. & Kumar, J. A. (2017). Machinability of hybrid metal matrix composite-A review. *Procedia Engineering, 174*, pp. 1110-1118. DOI: 10.1016/j.proeng.2017.01.264

[7] Chawla, K.K. 2012. *Composite Materials: Science and Engineering*, Springer Science & Business Media.

[8] Boothroyd, G. & Winston, A.K. (2011). *Fundamentals of Metal Machining and Machine Tools*, CRC Press.

[9] Poornachandiran, N., Pugazhenthi, R., Vijay Ananth, S., Krishnan, T.G. & Vairavel, M. (2020). Investigation of mechanical properties of Al6061 with reinforcement of SiC/B4C metal matrix composites. *AIP Conference Proceedings 2283*, 020113. DOI: 10.1063/5.0025004

[10] Jawalkar, C., Verma, A.S. & Suri, N. (2017). Fabrication of aluminum metal matrix composites with particulate reinforcement: a review. *Materials Today: Proceedings, 4*, pp. 2927-2936. DOI: 10.1016/j.matpr.2017.02.174

[11] Kala, H., Mer, K. & Kumar, S. (2014). A review on mechanical and tribological behaviors of stir cast aluminum matrix composites. *Procedia Materials Science, 6*, pp. 1951-1960. DOI: 10.1016/j.mspro.2014.07.229

[12] Sharma, V., Rao, P., Kumar, H. & Khan, M.Y. (2021). An experimental investigation ECM of titanium 6AL-4V-ELI alloy with different electrolytes. *Journal of University of Shanghai for Science and Technology, JUSST, 23*, pp. 292-303.

[13] Masooth, P.H.S., Bharathiraja, G., Jayakumar, V. & Palani, K. (2022). Analysis of machining characteristics in electrical discharge machining of SiC and Al_2O_3 reinforced AA6061 hybrid metal matrix composites using Taguchi and ANOVA techniques. *Materials Research Express, 9*, 046521. DOI: 10.1088/2053-1591/ac672d

[14] Ibrahim, A.F., Mousa, S.M. & Kareem Noori, D.A. (2022).

Investigation and optimization of machining parameters in electrochemical machining of aluminum metal matrix composites. *Periodicals of Engineering and Natural Sciences, 10*, pp. 48-59.

[15] Gugulothu, B., Satheesh Kumar, P.S., Srinivas, B., Ramakrishna, A. & Vijayakumar, S. (2021). Investigating the Material Removal Rate Parameters in ECM for Al 5086 Alloy-Reinforced Silicon Carbide/Flyash Hybrid Composites by Using Minitab-18. *Advances in Materials Sciences and Engineering 2021*, 2079811. DOI: 10.1155/2021/2079811

[16] Ahmadinia, O.F., Küçüktürk, G., Sucularli, F. & Gürün, H. (2022). Machinability of B4C-reinforced Al2014 metal matrix composites in electric discharge machining. *Revista De Metalurgia,* 58.

[17] Kannan, P.R., Periasamy, K., Pravin, P. & Vinod Kumaar, J.R. (2022). Anexperimental investigation of wire breakage and performance optimization of WEDM process on machining of recycled aluminium alloy metal matrix composite. *Materials Science-Poland, 40*, pp. 12-26. DOI: 10.2478/msp-2022-0030

[18] Mohankumar, V., Kapilan, S., Karthik, A., Bhuvaneshwaran, M., Santulli, C., Kumar, D.T., Palanisamy, S. & Fragassa, C. (2024). A Hybrid Design of Experiment Approach in Analyzing the Electrical Discharge Machining Influence on Stir Cast Al7075/B4C Metal Matrix Composites. *Metals, 14*, 205. DOI: 10.3390/met14020205

[19] Mandal, N., Hloch, S. & Das, A.K. (2022). Comparison of Maraging Steel Surface Integrity in Hybrid and Conventional Micro-ECDM Processes. *Materials, 15*, 4378. DOI: 10.3390/ma15134378

[20] Selvarasu, S., Subramanian, M. & Thangasamy, J. (2023). An effect of nano-SiC with different dielectric mediums on AZ61/7.5% B4C nanocomposites studied through electrical discharge machining and Taguchi based complex proportional assessment method. *Matéria (Rio de Janeiro), 28*, e20230058. DOI: 10.1590/1517-7076-RMAT-2023-0058

[21] Jabbar, A.A. & Mohd, A. (2023). Effect of Volume Percentage of Reinforcement on the Microstructure and Mechanical Properties of an Al6061-T6/SiC Surface Composite Fabricated Through Friction Stir Processing. *Advances in Science and Technology, 17*, pp. 247-257. DOI: 10.12913/22998624/161690

[22] Bharath, V., Nagaral, M., Auradi, V. & Kori, S.A. (2014). Preparation of 6061Al-Al_2O_3 MMC's by Stir Casting and Evaluation of Mechanical and Wear Properties. *Procedia Materials Science, 6*, pp. 1658-1667. DOI: 10.1016/j.mspro.2014.07.151

[23] Leela, B.N., Prasanna, N.D. & Balasubramanya, H.S. (2020). Mechanical and Wear Behavior of Al-6061 Aluminum Alloy Composites Subjected to B4C Particulates Produced using Stir Casting. *International Journal of Engineering Research & Technology, 8*, pp. 110-114

[24] Rao, V.R.K., Ramanaiah, N. & Sarcar, M.M.M. (2014). Fabrication and Investigation on Properties of TiC Reinforced Al7075 Metal Matrix Composites. *Applied Mechanics and Materials, 592-594*, pp. 349-353. DOI: 10.4028/www.scientific.net/AMM.592-594.349

[25] Ramanathan, A., Krishnan, P.K. & Muraliraja, R. (2019). A review on the production of metal matrix composites through stir casting – Furnace design, properties, challenges, and research opportunities. *Journal of Manufacturing Processes, 42*, pp. 213-245. DOI: 10.1016/j.jmapro.2019.04.017

[26] Abdulwahhab, A.B. & Ibrahim, A.F. (2025). Effect of Hybrid Composite Electrode (Cu/Cr/Wc/Ag) on Surface Integrity of Stainless Steel 304l Machined by EDM. *Management Systems in Production Engineering, 33*, pp. 136-143. DOI: 10.2478/mspe-2025-0014

[27] Rajput, V., Goud, M. & Suri, N.M. (2021). Electrochemical discharge machining: gas film electrochemical aspects, stability parameters, and research work. *Journal of the Electrochemical Society, 168*, 013503. DOI: 10.1149/1945-7111/abd516

[28] Mazza, B., Pedeferri, P. & Re, G. (1978). Hydrodynamic instabilities in electrolytic gas evolution. *Electrochimica Acta,* 23, 87-93. DOI: 10.1016/0013-4686(78)80102-9

[29] Wüthrich, R., Spaelter, U. & Bleuler, H. (2006). The current signal in spark-assisted chemical engraving (SACE): what does it tell us? *Journal of Micromechanics and Microengineering, 16*, 779. DOI: 10.1088/0960-1317/16/4/014

[30] Hourmand, M., Sarhan, A.A., Farahany, S. & Sayuti, M. (2019). Microstructure characterization and maximization of the material removal rate in nano-powder mixed EDM of Al-Mg_2Si metal matrix composite – ANFIS and RSM approaches. *The International Journal of Advanced Manufacturing Technology, 101*, pp. 2723-2737. DOI: 10.1007/s00170-018-3130-3

Safa M. Lafta (corresponding author)
ORCID ID: 0009-0007-5334-9168
Department of Production Engineering and Metallurgy
College of Engineering
University of Technology, Baghdad, Iraq
e-mail: pme.20.88@grad.uotecnology.edu.iq

Abbas F. Ibrahim
ORCID ID: 0000-0002-0223-3241
Department of Production Engineering and Metallurgy
College of Engineering
University of Technology, Baghdad, Iraq
e-mail: Abbas.F.Ibrahim@uotechnology.edu.iq